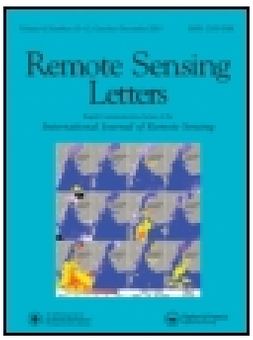

Remote Sensing Letters

ISSN: 2150-704X (Print) 2150-7058 (Online) Journal homepage: http://www.tandfonline.com/loi/trsl20

A marked point process for automated building detection from lidar point-clouds

Yongtao Yu, Jonathan Li, Haiyan Guan & Cheng Wang

To cite this article: Yongtao Yu, Jonathan Li, Haiyan Guan & Cheng Wang (2013) A marked point process for automated building detection from lidar point-clouds, Remote Sensing Letters, 4:11, 1127-1136, DOI: 10.1080/2150704X.2013.846487

To link to this article: http://dx.doi.org/10.1080/2150704X.2013.846487

Remote Sensing Letters, 2013
Vol. 4, No. 11, 1127–1136, http://dx.doi.org/10.1080/2150704X.2013.846487

A marked point process for automated building detection from lidar point-clouds

YONGTAO YU†, JONATHAN LI*†‡, HAIYAN GUAN† and CHENG WANG
†School of Information Science and Engineering, Xiamen University, Xiamen, Fujian 361005, China
‡Faculty of Environment, University of Waterloo, Waterloo, Ontario N2L 3G1, Canada

(*Received 9 July 2013; accepted 12 September 2013*)

This letter presents a novel algorithm for automated building detection from light detection and ranging (lidar) point-clouds. The algorithm takes advantage of a marked point process to model the locations of buildings and their geometries. A Bayesian paradigm is used to obtain a posterior distribution for the marked point process. A Reversible Jump Markov Chain Monte Carlo (RJMCMC) algorithm is implemented for simulating the posterior distribution. Finally, the maximum a posteriori (MAP) scheme is used to obtain an optimal building detection. The results obtained on a set of lidar point-clouds demonstrate the efficiency of the proposed algorithm in automated detection of buildings in complex residential areas.

1. Introduction

Since buildings are one of the most obvious features of a city or a rural area, geometric modelling of buildings becomes a fundamental part in a growing number of applications, ranging from urban planning, environmental impact assessment, cultural heritage protection, transportation management to disaster preparedness. To date, automatically detecting and modelling buildings from remotely sensed data has been a challenging topic in the fields of photogrammetry, remote sensing, and computer vision. Existing methods to building detection are time-consuming when processing large scenes containing hundreds of buildings. For example, in Ortner *et al.* (2007), 3 hours were required to automatically extract building outlines from images taken over an area of 200 m × 200 m in size. Therefore, automated and efficient methods to building detection from large scenes are highly in demand.

Light detection and ranging (lidar) technologies have been rapidly developed for the acquisition of geospatial information in recent years (Shan and Toth 2008). Due to the capability of lidar systems in directly measuring the surface topography accurately and densely without any geometrical distortions, the data scanned by these systems have become a leading source for automated extraction of various objects (e.g. buildings, trees, terrain, etc.) (Xu *et al.* 2007, Lafarge *et al.* 2008, Pu *et al.* 2011). Consequently, a variety of methods to building detection (Ma 2005, Zhang *et al.* 2006) from lidar point-clouds have been proposed in the literature. However, these methods suffered from high time complexities and high omission errors (e.g. omission error of up to

*Corresponding author. Email: junli@uwaterloo.ca

35% in Zhang *et al.* (2006)). Therefore, it is impractical to directly apply these methods to large scenes containing numerous buildings.

In this letter, we present a marked point process-based approach to building detection from lidar point-clouds. This is a stochastic and object-oriented method, which can efficiently process large scenes with unknown number of buildings and buildings with unknown sizes and adjust the boundaries of all the detected buildings within a short time. The idea behind the marked point process is to model the number and locations of buildings as point processes, to define their geometries as marks, and to attach a set of random parameters to each building. The proposed algorithm has been tested on a set of lidar point-clouds. The results demonstrate the efficiency and feasibility of the proposed algorithm in automatically detecting buildings.

2. Methodology

2.1 *Data model*

A lidar point-cloud is a collection of data points $\{(x_i, y_i, z_i); i = 1,2, \ldots n\}$, where n is the total number of data points. These data points can be re-originated as $Z = \{z_i = Z(x_i, y_i); i = 1,2, \ldots n, (x_i, y_i) \in \mathrm{D}\}$. From a spatial statistics point of view, Z can be considered as a collection of discrete samples on the ground points $\{(x_i, y_i); i = 1,2, \ldots n\}$ from a random function $Z(x, y)$ defined on domain D. On the other hand, Z can be characterized by a random field (RF), in which the collection of n georeferenced observations do not represent a sample of size n, but rather a sample of size one from an n-dimensional distribution (Schabenberger and Gotway 2005).

Consider an RF $Z = \{z_i = Z(x_i, y_i); i = 1,2, \ldots n, (x_i, y_i) \in \mathrm{D}\}$, from which a lidar point-cloud is sampled. In order to distinguish buildings from other objects, such as the ground and trees in Z, D is divided into three regions, i.e. $\mathrm{D} = \{\mathrm{D_g}, \mathrm{D_t}, \mathrm{D_b}\}$, where $\mathrm{D_g}$, $\mathrm{D_t}$, and $\mathrm{D_b}$ correspond to the ground, tree, and building regions, respectively, and $\mathrm{D_b} = \{\mathrm{W}_j; j = 1,2, \ldots k\}$, where W_j is the orthographic projection (or outline) of the jth building and k denotes the number of buildings. Assume that the elevations in these three regions are characterized by Gaussian distributions as follows:

$$p(z_i) = \begin{cases} \frac{1}{\sqrt{2\pi}\sigma_\mathrm{g}} \exp\left(-\frac{(z_i-\mu_\mathrm{g})^2}{2\sigma_\mathrm{g}^2}\right), (x_i, y_i) \in \mathrm{D_g} \\ \frac{1}{\sqrt{2\pi}\sigma_\mathrm{t}} \exp\left(-\frac{(z_i-\mu_\mathrm{t})^2}{2\sigma_\mathrm{t}^2}\right), (x_i, y_i) \in \mathrm{D_t} \\ \frac{1}{\sqrt{2\pi}\tau_j} \exp\left(-\frac{(z_i-\upsilon_j)^2}{2\tau_j^2}\right), (x_i, y_i) \in \mathrm{W}_j \end{cases}, \tag{1}$$

where μ_g, μ_t, υ_j, σ_g, σ_t, and τ_j are the means and standard deviations of Gaussian distributions for the elevations of the ground, trees, and the jth building, respectively.

Assume that all elevations are independent. Then, the joint distribution for the elevations in each object region is expressed as follows:

$$\begin{cases} p(Z_\mathrm{g}) = \Pi_{(x_i,y_i)\in \mathrm{D_g}} \frac{1}{\sqrt{2\pi}\sigma_\mathrm{g}} \exp\left(-\frac{(z_i-\mu_\mathrm{g})^2}{2\sigma_\mathrm{g}^2}\right), Z_\mathrm{g} = \left\{z_i; (x_i, y_i) \in \mathrm{D_g}, i \in \{1, 2, \ldots n\}\right\} \\ p(Z_\mathrm{t}) = \Pi_{(x_i,y_i)\in \mathrm{D_t}} \frac{1}{\sqrt{2\pi}\sigma_\mathrm{t}} \exp\left(-\frac{(z_i-\mu_\mathrm{t})^2}{2\sigma_\mathrm{t}^2}\right), Z_\mathrm{t} = \{z_i; (x_i, y_i) \in \mathrm{D_t}, i \in \{1, 2, \ldots n\}\} \\ p(Z_\mathrm{b}) = \Pi_{\mathrm{W}_j\in \mathrm{D_b}} \Pi_{(x_i,y_i)\in \mathrm{W}_j} \frac{1}{\sqrt{2\pi}\tau_j} \exp\left(-\frac{(z_i-\upsilon_j)^2}{2\tau_j^2}\right), Z_\mathrm{b} = \{z_i; (x_i, y_i) \in \mathrm{D_b}, i \in \{1, 2, \ldots n\}\}. \end{cases} \tag{2}$$

2.2 *Building model*

A building is composed of one or multiple simple shapes with rectangular footprints. In this letter, a building is characterized by a cuboid with an attribute vector (u, v, h, l, w, α), where (u, v) is the centre of the orthographic projection of the cuboid, and h, l, w, and α are the height, length, width, and orientation of the cuboid, respectively. In addition, υ and τ are introduced to represent the mean and standard deviation of a Gaussian distribution that models the distribution of the height h.

In this letter, the attribute vectors for all buildings are modelled with a marked point process, in which the locations of building centres $G = \{(u_j, v_j); j = 1,2, \ldots k\}$ is characterized by a homogeneous Poisson point process, where k, denoting the number of buildings, follows a Poisson distribution and (u_j, v_j) distributes on D uniformly. The marks associated with the centres, denoted by $M = \{(l_j, w_j, \alpha_j, \upsilon_j, \tau_j); j = 1,2, \ldots k\}$, in the point process are the geometric attributes of the buildings.

2.3 *Bayesian model*

The parameter set of the buildings is denoted by $B = \{\mathrm{G}, \mathrm{M}, k\}$. It can be rewritten as $B = \{\mathrm{G}, l, w, \alpha, \upsilon, \tau\}$, where $l = \{l_j; j = 1,2, \ldots k\}$, $w = \{w_j; j = 1,2, \ldots k\}$, $\alpha = \{\alpha_j; j = 1,2, \ldots k\}$, $\upsilon = \{\upsilon_j; j = 1,2, \ldots k\}$, and $\tau = \{\tau_j; j = 1,2, \ldots k\}$. By Bayesian paradigm, the posterior distribution of the parameter set conditional on a given point-cloud is expressed as follows:

$$P(\mathrm{B}|\mathrm{Z}) \propto P(\mathrm{Z}|\mathrm{B})P(\mathrm{B}), \tag{3}$$

where $P(\cdot)$ denotes the probability, and the likelihood $P(\mathrm{Z}|\mathrm{B})$ is defined as

$$P(\mathrm{Z}|\mathrm{B}) = P(\mathrm{Z}|\mathrm{G}, \mathrm{M}, k) = P(Z_\mathrm{g})P(Z_\mathrm{t})P(Z_\mathrm{b}|\mathrm{G}, \mathrm{M}, k), \tag{4}$$

and

$$P(\mathrm{B}) = P(\mathrm{G}|k)P(\mathrm{l}|k)P(w|k)P(\alpha|k)P(\upsilon|k)P(\tau|k)P(k). \tag{5}$$

Assume that the centres and orientations uniformly distribute on D and $(-\pi/2, \pi/2]$, respectively; the prior distribution of the parameter k is assumed to follow a Poisson distribution with mean λ (Stoyan *et al.* 1995), and other parameters are assumed to be Gaussian distributions.

2.4 *Simulation and optimization*

In order to simulate the posterior distribution in equation (3), the Reversible Jump Markov Chain Monte Carlo (RJMCMC) (Green 1995) algorithm is implemented. The flow chart of the proposed algorithm is shown in figure 1. The operations proposed in the scheme include (1) updating building model parameters in $M = \{\mathrm{l}, w, \alpha, \upsilon, \tau\}$, (2) moving the centres in G, and (3) birth or death of a building. Once the operations are determined, the scheme can be designed as follows.

(1) Initialization. Set the initial number of buildings, taking $k^0 = 1$, for simplicity. Here, the superscript '0' represents the initial case. Set the initial value of the

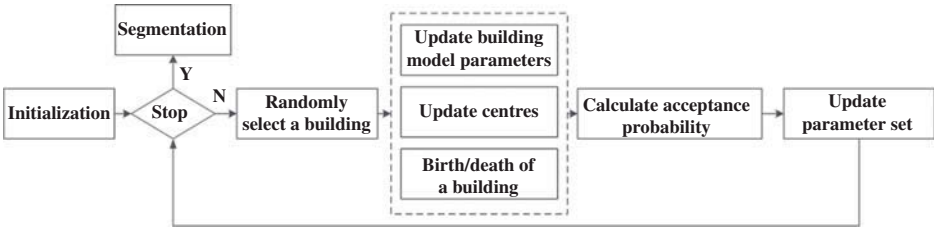

Figure 1. Flow chart of the proposed algorithm.

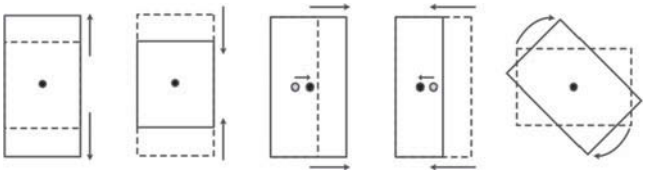

Figure 2. Transformations: (*a*) centre-based dilation, (*b*) centre-based shrinkage, (*c*) edge-based dilation, (*d*) edge-based shrinkage, and (*e*) centre-based rotation.

parameter vector $\mathrm{M}^0 = (\mathrm{l}^0, w^0, \alpha^0, \upsilon^0, \tau^0)$, which are drawn from their appropriate distributions. Set the initial locations of buildings $\mathrm{G}^0 = (\mathrm{u}^0, \mathrm{v}^0)$, which are uniformly drawn on D. And set the maximum iterations T_m.

(2) Updating building model parameters. As shown in figure 2, we consider five types of transformations: centre-based dilation, centre-based shrinkage, edge-based dilation, edge-based shrinkage, and centre-based rotation. For a selected building model parameters $\boldsymbol{M}_j^{(t-1)} = (l_j^{(t-1)}, w_j^{(t-1)}, \alpha_j^{(t-1)}, \upsilon_j^{(t-1)}, \tau_j^{(t-1)}), j \in \{1,2, \ldots k\}$ in the tth iteration, draw a proposal $\boldsymbol{M}_j^* = (l_j^*, w_j^*, \alpha_j^*, \upsilon_j^*, \tau_j^*)$ from $N(\boldsymbol{M}_j^{(t-1)}, \boldsymbol{\varepsilon})$, where $N(\mu, \sigma)$ represents a Gaussian distribution with mean μ and standard deviation σ, and $\boldsymbol{\varepsilon} = (\varepsilon_\mathrm{l}, \varepsilon_\mathrm{w}, \varepsilon_\alpha, \varepsilon_\upsilon, \varepsilon_\tau)$, where ε_l, ε_w, ε_α, ε_υ, and ε_τ are the standard deviations of Gaussian distributions for the length, width, orientation, height mean, and height standard deviation of the building model parameters. Then calculate the acceptance probability for the proposal as follows:

$$r_\mathrm{B}(B_j^*, B_j^{(t-1)}) = \min\left(1, \frac{P(\mathrm{Z}_{\mathrm{W}_j^*}|B_j^*)P(B_j^*)\exp\left(\frac{n_j^*}{N_j^*}\right)}{P(\mathrm{Z}_{\mathrm{W}_j^{(t-1)}}|B_j^{(t-1)})P(B_j^{(t-1)})\exp\left(\frac{n_j^{(t-1)}}{N_j^{(t-1)}}\right)}\right), \tag{6}$$

where $B_j^{(t\text{-}1)}$ and B_j^* denote the parameter set of building j before and after updating, $\mathrm{W}_j^{(t-1)}$ and W_j^* denote the region of building j before and after updating, $\mathrm{Z}_{\mathrm{W}_j^{(t-1)}} = \{z_i; (x_i, y_i) \in \mathrm{W}_j^{(t-1)}, i \in \{1, 2, \ldots n\}\}$ and $\mathrm{Z}_{\mathrm{W}_j^*} = \{z_i; (x_i, y_i) \in \mathrm{W}_j^*, i \in \{1, 2, \ldots n\}\}$ represent the point sets corresponding to building j before and after updating, n_j is the number of data points within W_j that match the prior model, and N_j is the total number of data points within W_j. Finally, accept

the proposal if the acceptance probability exceeds a constant false alarm ratio (CFAR) p_{f}, i.e.

$$B_j^{(t)} = \begin{cases} B_j^*, & r_{\mathrm{B}} \geq p_{\mathrm{f}} \\ B_j^{(t-1)}, & r_{\mathrm{B}} < p_{\mathrm{f}} \end{cases}. \tag{7}$$

(3) Updating centres. For a selected centre $\boldsymbol{G}_j^{(t-1)} = (u_j^{(t-1)}, v_j^{(t-1)})$, $j \in \{1,2, \ldots k\}$ in the tth iteration, propose a new centre $\boldsymbol{G}_j^* = (u_j^*, v_j^*)$ by uniformly drawing a point from W_j. There are two non-building classes: ground and tree; therefore, there are four combinations for calculating the acceptance probability as follows:

$$r_{\mathrm{B}}^1\left(B_j^*, B_j^{(t-1)}\right) = \min\left(1, \frac{P(\mathrm{Z}_{\mathrm{W}_j^*-\mathrm{W}_j}|\upsilon_j^*, \tau_j^*)P(\mathrm{Z}_{\mathrm{W}_j-\mathrm{W}_j^*}|\mu_{\mathrm{g}}, \sigma_{\mathrm{g}})P(B_j^*)\exp\left(\frac{n_j^*}{N_j^*}\right)}{P(\mathrm{Z}_{\mathrm{W}_j^*-\mathrm{W}_j}|\mu_{\mathrm{g}}, \sigma_{\mathrm{g}})P(\mathrm{Z}_{\mathrm{W}_j-\mathrm{W}_j^*}|\upsilon_j, \tau_j)P\left(B_j^{(t-1)}\right)\exp\left(\frac{n_j^{(t-1)}}{N_j^{(t-1)}}\right)}\right), \tag{8}$$

$$r_{\mathrm{B}}^2\left(B_j^*, B_j^{(t-1)}\right) = \min\left(1, \frac{P(\mathrm{Z}_{\mathrm{W}_j^*-\mathrm{W}_j}|\upsilon_j^*, \tau_j^*)P(\mathrm{Z}_{\mathrm{W}_j-\mathrm{W}_j^*}|\mu_{\mathrm{t}}, \sigma_{\mathrm{t}})P(B_j^*)\exp\left(\frac{n_j^*}{N_j^*}\right)}{P(\mathrm{Z}_{\mathrm{W}_j^*-\mathrm{W}_j}|\mu_{\mathrm{g}}, \sigma_{\mathrm{g}})P(Z_{\mathrm{W}_j-\mathrm{W}_j^*}|\upsilon_j, \tau_j)P\left(B_j^{(t-1)}\right)\exp\left(\frac{n_j^{(t-1)}}{N_j^{(t-1)}}\right)}\right), \tag{9}$$

$$r_{\mathrm{B}}^3\left(B_j^*, B_j^{(t-1)}\right) = \min\left(1, \frac{P(\mathrm{Z}_{\mathrm{W}_j^*-\mathrm{W}_j}|\upsilon_j^*, \tau_j^*)P(\mathrm{Z}_{\mathrm{W}_j-\mathrm{W}_j^*}|\mu_{\mathrm{g}}, \sigma_{\mathrm{g}})P(B_j^*)\exp\left(\frac{n_j^*}{N_j^*}\right)}{P(\mathrm{Z}_{\mathrm{W}_j^*-\mathrm{W}_j}|\mu_{\mathrm{t}}, \sigma_{\mathrm{t}})P(\mathrm{Z}_{\mathrm{W}_j-\mathrm{W}_j^*}|\upsilon_j, \tau_j)P\left(B_j^{(t-1)}\right)\exp\left(\frac{n_j^{(t-1)}}{N_j^{(t-1)}}\right)}\right), \tag{10}$$

$$r_{\mathrm{B}}^4\left(B_j^*, B_j^{(t-1)}\right) = \min\left(1, \frac{P(\mathrm{Z}_{\mathrm{W}_j^*-\mathrm{W}_j}|\upsilon_j^*, \tau_j^*)P(\mathrm{Z}_{\mathrm{W}_j-\mathrm{W}_j^*}|\mu_{\mathrm{t}}, \sigma_{\mathrm{t}})P(B_j^*)\exp\left(\frac{n_j^*}{N_j^*}\right)}{P(\mathrm{Z}_{\mathrm{W}_j^*-\mathrm{W}_j}|\mu_{\mathrm{t}}, \sigma_{\mathrm{t}})P(\mathrm{Z}_{\mathrm{W}_j-\mathrm{W}_j^*}|\upsilon_j, \tau_j)P\left(B_j^{(t-1)}\right)\exp\left(\frac{n_j^{(t-1)}}{N_j^{(t-1)}}\right)}\right), \tag{11}$$

where $\mathrm{Z}_{\mathrm{W}_j^*-\mathrm{W}_j} = \{z_i; (x_i, y_i) \in \mathrm{W}_j^* \wedge (x_i, y_i) \notin \mathrm{W}_j, i \in \{1, 2, \ldots n\}\}$ and $\mathrm{Z}_{\mathrm{W}_j-\mathrm{W}_j^*}$ is defined similarly. Then, accept the proposal if one of the two following conditions meets: (1) $r_{\mathrm{B}}^1 \geq p_{\mathrm{f}}$ and $r_{\mathrm{B}}^3 \geq p_{\mathrm{f}}$ or (2) $r_{\mathrm{B}}^2 \geq p_{\mathrm{f}}$ and $r_{\mathrm{B}}^4 \geq p_{\mathrm{f}}$.

(4) Birth or death of a building. Let the probability of proposing a birth or death operation be b_k or d_k, respectively, where k denotes the current number of buildings. For a birth operation, draw the centre $\boldsymbol{G}_{k+1}^* = (u_{k+1}^*, v_{k+1}^*)$ from $\mathrm{D} - \mathrm{D}_{\mathrm{b}}$ uniformly and draw the parameters $\boldsymbol{M}_{k+1}^* = (l_{k+1}^*, w_{k+1}^*, \alpha_{k+1}^*, \upsilon_{k+1}^*, \tau_{k+1}^*)$ for the new building from their prior distributions. According to the RJMCMC scheme (Green 1995), the acceptance probability for the birth operation is written as

$$r_{\mathrm{b}}(\mathrm{B}^*, \mathrm{B}) = \min\left(1, \frac{P(\mathrm{Z}|\mathrm{B}^*)P(\mathrm{B}^*)j_{b_k}(\mathrm{B}^*)}{P(\mathrm{Z}|\mathrm{B})P(\mathrm{B})j_{d_{k+1}}(\mathrm{B})P(\mathrm{B}^*_{k+1})}\left|\frac{\partial(\mathrm{B}^*)}{\partial(\mathrm{B}, \mathrm{B}^*_{k+1})}\right|\right), \tag{12}$$

where $j_{b_k}(\mathrm{B}^*) = b_k, j_{d_{k+1}}(\mathrm{B}) = \frac{d_{k+1}}{k+1}, \frac{P(\mathrm{B}^*)}{P(\mathrm{B})P(\mathrm{B}^*_{k+1})} = \frac{P(k+1)}{P(k)} = \frac{\lambda}{k+1}, \left|\frac{\partial(\mathrm{B}^*)}{\partial(\mathrm{B}, \mathrm{B}^*_{k+1})}\right| = 1.$
For simplicity, let $d_{k+1} = \lambda b_k$, then equation (12) can be rewritten as

$$r_{\mathrm{b}}(\mathrm{B}^*, \mathrm{B}) = \min\left(1, \frac{P(\mathrm{Z}|\mathrm{B}^*)}{P(\mathrm{Z}|\mathrm{B})}\right). \tag{13}$$

Since there are two non-building classes, there are two combinations for calculating the acceptance probability as follows:

$$r_{\mathrm{bg}}(\mathrm{B}^*, \mathrm{B}) = \min\left(1, \frac{\prod_{(x_i,y_i)\in \mathrm{W}_{k+1}} \frac{1}{\sqrt{2\pi}\tau^*_{k+1}} \exp\left(-\frac{(z_i-\upsilon^*_{k+1})^2}{2(\tau^*_{k+1})^2}\right)}{\prod_{(x_i,y_i)\in \mathrm{W}_{k+1}} \frac{1}{\sqrt{2\pi}\sigma_{\mathrm{g}}} \exp\left(-\frac{(z_i-\mu_{\mathrm{g}})^2}{2\sigma^2_{\mathrm{g}}}\right)}\right), \tag{14}$$

$$r_{\mathrm{bt}}(\mathrm{B}^*, \mathrm{B}) = \min\left(1, \frac{\prod_{(x_i,y_i)\in \mathrm{W}_{k+1}} \frac{1}{\sqrt{2\pi}\tau^*_{k+1}} \exp\left(-\frac{(z_i-\upsilon^*_{k+1})^2}{2(\tau^*_{k+1})^2}\right)}{\prod_{(x_i,y_i)\in \mathrm{W}_{k+1}} \frac{1}{\sqrt{2\pi}\sigma_{\mathrm{t}}} \exp\left(-\frac{(z_i-\mu_{\mathrm{t}})^2}{2\sigma^2_{\mathrm{t}}}\right)}\right). \tag{15}$$

Accept the new building if $r_{\mathrm{bg}} \geq p_{\mathrm{f}}$ and $r_{\mathrm{bt}} \geq p_{\mathrm{f}}$.
The acceptance probability for the death operation is as follows:

$$r_{\mathrm{d}}(\mathrm{B}^*, \mathrm{B}) = \min\left(1, \frac{P(\mathrm{Z}|\mathrm{B})}{P(\mathrm{Z}|\mathrm{B}^*)}\right). \tag{16}$$

After the maximum iteration T_{m}, the maximum a posteriori (MAP) criterion is used to obtain the final segmentation:

$$\mathrm{B} = \arg\{\max(P(\mathrm{B}|\mathrm{Z}))\}. \tag{17}$$

3. Experimental results and discussion

3.1 *Study area and data set*

The data sets used in our experiments are the 'Downtown Toronto' and 'Vaihingen' data sets from ISPRS Commission III, WG III/4. The 'Downtown Toronto' data set covers an area of about 1.45 km^2 in the central area of Toronto in Canada (figure 3(*a*)). The data were captured by the Microsoft Vexcel's UltraCam-D (UCD) camera and the Optech airborne laser scanner ALTM-ORION M. The 'Vaihingen' data set was captured by Leica ALS50 over Vaihingen in Germany (figure 3(*b*)). We selected four topographic lidar point-clouds covering areas with buildings from the above two data sets. Figure 4 shows the test data I containing two point-clouds selected from the 'Downtown Toronto' data set, and figure 5 shows the test data II containing two point-clouds selected from the 'Vaihingen' data set. The colours represent elevation variations.

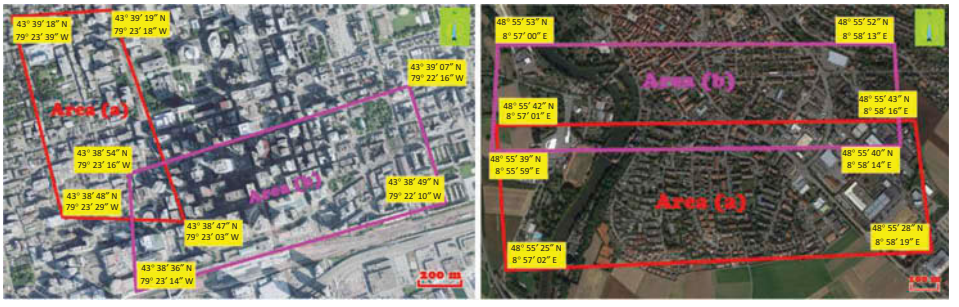

(*a*) (*b*)

Figure 3. Overview of the study areas: (*a*) Downtown Toronto and (*b*) Vaihingen.

(*a*) (*b*)

Figure 4. Test data I: point-clouds (*a*) and (*b*) from 'Downtown Toronto' data set.

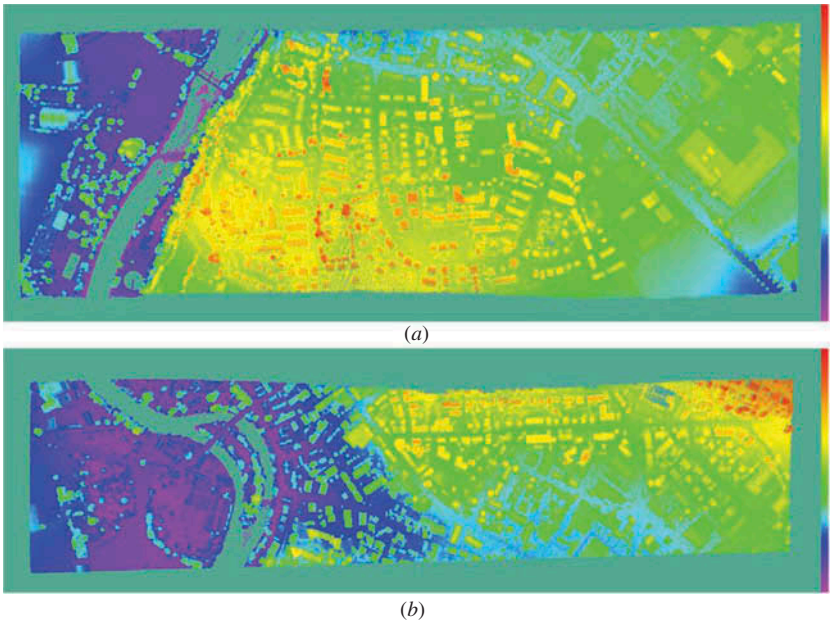

(*a*)

(*b*)

Figure 5. Test data II: point-clouds (*a*) and (*b*) from 'Vaihingen' data set.

3.2 *Detection results*

Figures 6 and 7 show the distributions of detected building outlines after we apply the proposed algorithm to the four point-clouds. For test data I, there are 130 and 153 detected building outlines for the two point-clouds, respectively. For test data II, there are 263 and 290 detected building outlines for the two point-clouds, respectively. The detected building outlines are overlaid on test data I and test data II, respectively, for visual inspection in order to evaluate the accuracy of the proposed algorithm (figures 6 and 7). The detected results illustrate that the proposed algorithm detects rectangular shape buildings quite well. However, for some non-rectangular or irregular shape buildings, the proposed algorithm does not work very well. Some of these buildings were either partially detected or detected as more than one segment. In addition, for some small buildings that are hidden in big trees, the proposed algorithm fails to detect them. To accurately evaluate the detection results, seven indices were used for

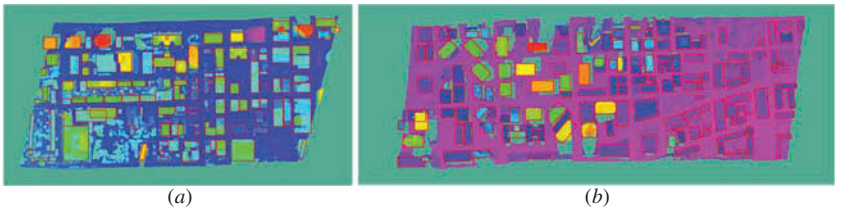

(*a*) (*b*)

Figure 6. Detected building outlines (red rectangles) of test data I (*a*) and (*b*).

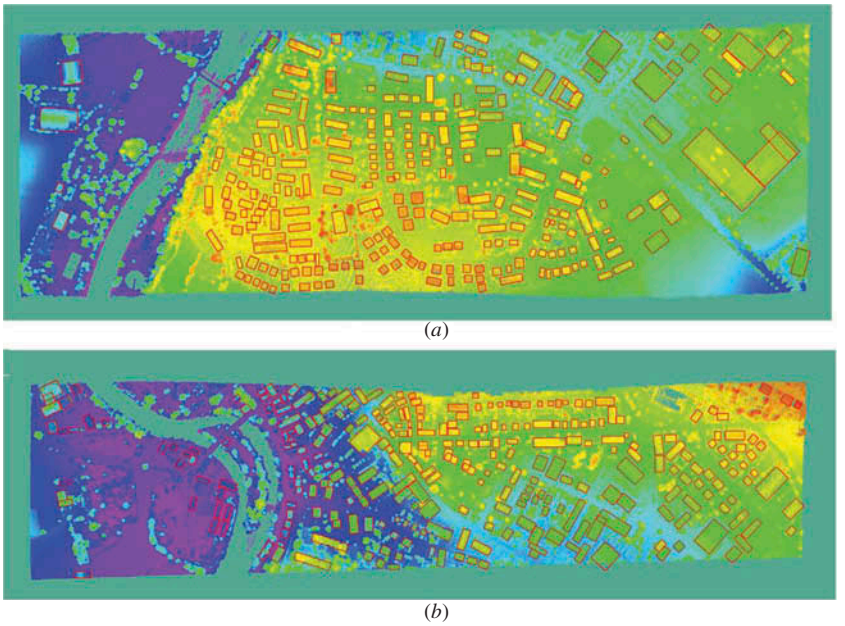

(*a*)

(*b*)

Figure 7. Detected building outlines (red rectangles) of test data II (*a*) and (*b*).

Table 1. Object-based evaluation results in percentage for the test data.

Lidar data	C_m	C_r	Q_l	M_d	D_o	C_{rd}	C_{rr}
Test data I(*a*)	96.97	98.46	95.52	3.08	3.08	2.31	6.92
Test data I(*b*)	96.77	98.04	94.94	5.23	11.76	5.88	5.23
Test data II(*a*)	96.23	96.96	93.41	2.28	3.42	1.90	5.70
Test data II(*b*)	94.50	94.83	89.87	3.45	6.55	3.10	6.21
Average	96.12	97.07	93.44	3.51	6.20	3.30	6.02

object-based evaluation (Awrangjeb *et al.* 2012): (1) *completeness* (C_m), (2) *correctness* (C_r), (3) *quality* (Q_l), (4) *multiple detection rate* (M_d), (5) *detection overlap rate* (D_o), (6) *detection cross-lap rate* (C_{rd}), and (7) *reference cross-lap rate* (C_{rr}). The evaluation results are listed in table 1. On average, 93.44% quality is achieved with 96.12% completeness and 97.07% correctness. The best performance was found in test data I(*a*). Therefore, the proposed algorithm performs quite well in detecting buildings from large-scene lidar point-clouds.

The proposed algorithm is developed using *C++* running on an Intel(R) Core(TM) i5 computer. The processing time for the four point-clouds, which contain 1,755,589 points; 1,928,393 points; 3,775,182 points; and 3,582,656 points, respectively, are 49 s, 51 s, 77 s, and 85 s, respectively. The computation burdens for updating building model parameters, updating centres, and birth or death of a building account for 5%, 35%, and 60%, respectively.

4. Conclusions

In this letter, we have proposed a novel algorithm for automated building detection from lidar point-clouds. The algorithm was based on a marked point process of rectangles and Bayesian inference. By using marked point processes, the algorithm can process large scenes containing unknown number of buildings and buildings with unknown sizes. Furthermore, the algorithm overcomes the limitations of the existing algorithms in time complexity and detection quality. The proposed algorithm can process a large point-cloud containing millions of points and hundreds of buildings within several minutes, and the average detection quality lies above 93%. In addition, instead of processing lidar point-clouds on a point-by-point basis towards building detection, the algorithm processes data points in and out of detected outlines simultaneously on an object-oriented basis. The building detection results demonstrate the efficiency and feasibility of the proposed algorithm in automatically detecting buildings from large-scene lidar point-clouds.

Acknowledgements

The authors would like to acknowledge the provision of the Downtown Toronto data set by Optech Inc., First Base Solutions Inc., GeoICT Lab at York University, and ISPRS WG III/4. The Vaihingen data set was provided by the German Society for Photogrammetry, Remote Sensing, and Geoinformation (DGPF).

References

Awrangjeb, M., Zhang, C. and Fraser, C.S., 2012, Building detection in complex scenes thorough effective separation of buildings from trees. *Photogrammetric Engineering & Remote Sensing*, **78**, pp. 729–745.

Green, J., 1995, Reversible jump Markov chain Monte Carlo computation and Bayesian model determination. *Biometrika*, **82**, pp. 711–732.

Lafarge, F., Descombes, X., Zerubia, J. and Pierrot-Deseilligny, M., 2008, Automatic building extraction from DEMs using an object approach and application to the 3D-city modeling. *ISPRS Journal of Photogrammetry and Remote Sensing*, **63**, pp. 365–381.

Ma, R., 2005, DEM generation and building detection from LiDAR data. *Photogrammetric Engineering and Remote Sensing*, **71**, pp. 847–854.

Ortner, M., Descombes, X. and Zerubia, J., 2007, Building outline extraction from digital elevation models using marked point processes. *International Journal of Computer Vision*, **72**, pp. 107–132.

Pu, S., Rutzinger, M., Vosselman, G. and Elberink, S.O., 2011, Recognizing basic structures from mobile laser scanning data for road inventory studies. *ISPRS Journal of Photogrammetry and Remote Sensing*, **66**, pp. S28–S39.

Schabenberger, O. and Gotway, C.A., 2005, *Statistical Methods for Spatial Data Analysis* (Boca Raton, FL: Chapman & Hall/CRC).

Shan, J. and Toth, C., 2008, *Topographic Laser Ranging and Scanning: Principles and Processing* (Boca Raton, FL: CRC Press).

Stoyan, A., Kendall, W.S. and Mecke, J., 1995, *Stochastic Geometry and Its Applications* (New York: Wiley).

Xu, H., Gossett, N. and Chen, B., 2007, Knowledge and heuristic-based modeling of laser-scanned trees. *ACM Transactions on Graphics*, **26**, pp. 19:1–13.

Zhang, K., Yan, J. and Chen, S.C., 2006, Automatic construction of building footprints from airborne LiDAR data. *IEEE Transactions on Geoscience and Remote Sensing*, **44**, pp. 2523–2533.